AGU PUBLICATIONS

Geophysical Research Letters

RESEARCH LETTER
10.1002/2014GL062569

Key Points:
- New estimation of vertical velocity derived from an observational-based approach
- QG-vertical velocities can sustain net primary production in the Gulf Stream
- The same methodology can be applied to other regions of the Global Ocean

Supporting Information:
- Text S1
- Text S2

Correspondence to:
A. Pascual,
ananda.pascual@imedea.uib-csic.es

Citation:
Pascual, A., S. Ruiz, B. Buongiorno Nardelli, S. Guinehut, D. Iudicone, and J. Tintoré (2015), Net primary production in the Gulf Stream sustained by quasi-geostrophic vertical exchanges, *Geophys. Res. Lett.*, *42*, doi:10.1002/2014GL062569.

Received 19 NOV 2014
Accepted 20 DEC 2014
Accepted article online 28 DEC 2014

Net primary production in the Gulf Stream sustained by quasi-geostrophic vertical exchanges

Ananda Pascual[1], Simón Ruiz[1], Bruno Buongiorno Nardelli[2,3], Stéphanie Guinehut[4], Daniele Iudicone[5], and Joaquín Tintoré[1,6]

[1]Instituto Mediterráneo de Estudios Avanzados, IMEDEA(CSIC-UIB), Majorca, Spain, [2]Istituto di Scienze dell'Atmosfera e del Clima, Rome, Italy, [3]Istituto per l'Ambiente Marino Costiero, Naples, Italy, [4]Collecte Localisation Satellites, Ramonville-Ste Agne, France, [5]Stazione Zoologica Anton Dohrn, Naples, Italy, [6]Balearic Islands Coastal Observing and Forecasting System, SOCIB, Majorca, Spain

Abstract We analyze 12 years of mesoscale vertical motion derived from an observation-based product in the top 1000 m of the North West Atlantic Ocean. Vertical velocities (O(10 m d^{-1})) associated with Gulf Stream instabilities consist of alternating cells of upwelling and downwelling. Here we show that the magnitude of the vertical motions decays exponentially southward with an *e*-folding length scale that is informative on the dynamics of the system. We further investigate the impact of the vertical supply of nutrients about phytoplankton growth with a conceptual model incorporating the mean effect of nutrient distribution, quasi-geostrophic dynamics, and Ekman suction/pumping. Results confirm that the mean effect of mesoscale vertical velocity variability alone can sustain observed levels of net primary production in the immediate vicinity of the Gulf Stream, while other mechanisms, including horizontal advection and submesoscale dynamics, need to be considered when moving toward the subtropical gyre.

1. Introduction

Mesoscale oceanic structures drive intense horizontal and vertical motions that are known to affect biological processes [*McGillicuddy et al*., 1998; *Rodríguez et al*., 2001; *Gaube et al*., 2014]. In particular, frontal areas are characterized by high vertical velocities, which can significantly contribute to nutrient replenishment in the euphotic zone [*Mahadevan*, 2014]. This nutrient enrichment can, in turn, enhance phytoplankton growth and influence marine ecosystems across multiple trophic levels. Significant uncertainty still exists, however, in our understanding of the net effect of mesoscale variability on water mass formation, mean-flow interactions, biochemical tracer redistribution, and the consequent marine ecosystem response.

Moreover, the relative importance of how various mesoscale physical/biological mechanisms affect marine ecosystems remains hotly debated. A wide range of mechanisms and hypotheses has been discussed, starting from conceptual models such as eddy pumping due to the vertical uplift of the upper thermocline associated with eddy intensification or decay [*Franks et al*., 1986; *McGillicuddy et al*., 1998; *Siegel et al*., 1999; *Mahadevan et al*., 2012], eddy-induced Ekman pumping generated by spatial variations in wind stress resulting from eddy surface currents [*Martin and Richards*, 2001; *McGillicuddy et al*., 2007; *Benítez-Barrios et al*., 2011; *Gaube et al*., 2013, 2014], and eddy advection of phytoplankton and nutrients by the trapping of fluid within the eddy interior [*Gruber et al*., 2011; *Gaube et al*., 2014] and around the eddy periphery [*Siegel et al*., 2008; *Chelton et al*., 2011]. More advanced analyses based on both modeling and observational approaches have clearly indicated that overly simplified models (i.e., mostly placing maximum vertical exchanges at the center of mesoscale structures) are not able to accurately represent the three-dimensional mesoscale flow field, stressing the fundamental role played by quasi-geostrophic and semigeostrophic dynamics [*Pollard and Regier*, 1992; *Naveira Garabato et al*., 2001; *Gonzalez-Quiros et al*., 2004; *Ruiz et al*., 2009; *Buongiorno Nardelli et al*., 2012; *Pidcock et al*., 2013]. They have also indicated new mechanisms potentially modulating vertical exchanges inside mesoscale oceanic eddies, such as vortex Rossby waves [*Buongiorno Nardelli*, 2013], and submesoscale pumping [e.g., *Lévy et al*., 2001; *Mahadevan and Tandon*, 2006; *Viúdez and Claret*, 2009; *Calil and Richards*, 2010].

Although relatively intense vertical exchanges in the oceans are associated with mesoscale structures, they are generally 4 orders of magnitude smaller than horizontal exchanges. Consequently, in situ observations

©2014. American Geophysical Union. All Rights Reserved.

of mesoscale vertical motions are difficult to obtain [*Klein and Lapeyre*, 2009]. Therefore, a common technique used to infer vertical velocity is based on the solution of the quasi-geostrophic (QG hereinafter) Omega equation, which has been typically applied in individual field campaigns [*Tintoré et al*., 1991; *Allen et al*., 2001; *Gomis et al*., 2001; *Buongiorno Nardelli et al*., 2001; *Rodríguez et al*., 2001; *Pascual et al*., 2004; *Pidcock et al*., 2013].

In this context, our goal is to investigate the impact of the vertical exchange associated with mesoscale dynamics on nutrient availability for phytoplankton growth across the North West Atlantic Ocean. This is achieved by diagnosing the vertical exchanges associated with QG dynamics, as derived from an innovative approach that uses a global observation-based product (ARMOR3D). We further compare satellite-based estimates of Net Primary Production with estimates obtained by applying a simple analytical model proposed by *Lathuiliere et al*. [2011] (hereafter referred to as L11) to the observations. This conceptual model considers the mean effect of nutrient (nitrate) distribution, (sub) mesoscale dynamics, and Ekman suction/pumping, focusing on a range of possible biological regimes (namely consideration of the effect of different mortality and remineralization rates within the euphotic layer). The underlying hypothesis is that upward mesoscale vertical motions will inject nutrients from the subsurface layer to the surface euphotic zone, stimulating phytoplankton growth as a result of the consumption of upwelled nutrients. On the other hand, mesoscale downwelling exports phytoplankton out of the euphotic zone. The model indicates that in oligotrophic gyres, the injection of nutrients will dominate and therefore a net increase of primary production is expected due to the impact of mesoscale turbulence, whereas in coastal upwelling systems phytoplankton export will be the dominant mechanism in response to eddy pumping, in agreement with *Gruber et al*. [2011].

2. Data and Methods

2.1. Temperature, Salinity, and Geostrophic Currents Synthetic Fields

We use a Global Ocean observation-based product, referred to as ARMOR3D, which combines satellite estimates of sea surface temperature, sea level anomalies, and mean dynamic topography with in situ measurements of temperature and salinity to produce a multivariate ocean state estimation [*Guinehut et al*., 2004, 2012]. Steric height and derived geostrophic currents are computed from the temperature and salinity fields using the thermal wind equation method, by using the altimetric height as a surface reference level in the integration.

The validity of this simple approach has been evaluated by comparison with in situ observations and model reanalysis [*Mulet et al*., 2012]. In the upper 1000 m, velocities estimated from the ARMOR3D fields are highly correlated with measurements made by the RAPID-MOCHA current meters [*Cunningham et al*., 2007]. Away from the boundaries, where the ocean is largely geostrophic and hydrostatic, and therefore the thermal wind balance is an excellent approximation, errors have been shown to be less than 10%. Further, comparison of the derived current field with the 3-D velocities from a Mercator-Ocean reanalysis [*Ferry et al*., 2010; *Lique et al*., 2011] resulted in similar skill in reproducing the amplitude and variability of in situ current observations in the Atlantic Ocean.

ARMOR3D fields used in this study are computed on a monthly basis on a 1/3° Mercator horizontal grid from the surface down to 1500 m depth on 24 vertical levels, spanning the 12 year time period 1998–2009.

2.2. Biogeochemical Data

Satellite-based estimates of net primary production (NPP), defined as the difference of the total carbon fixed into organic matter by photosynthesis minus the carbon respired, were downloaded from http://www.science.oregonstate.edu/ocean.productivity/. Because significant differences exist between estimates of NPP, three different products were used: the Vertically Generalized Production Model (VGPM), the "Eppley" version of the VGPM (both described in *Behrenfeld and Falkowski* [1997], and the recent carbon-based production model [*Westberry et al*., 2008]. The fields are estimated on a 1/6° regular grid with monthly temporal resolution covering the 1998–2009 period.

Nitrate concentrations at the base of the euphotic layer were extracted from the World Ocean Atlas (WOA) climatology [*Boyer et al*., 2009]. The nitrate concentrations were subsequently interpolated to the spatial grid on which the ARMOR3D product is produced and spatially averaged.

©2014. American Geophysical Union. All Rights Reserved.

2.3. Computation of Vertical Velocity

The vertical component of the velocity field (henceforth referred to as QG-w) is estimated from the quasi-geostrophic (QG) omega equation, used here in the Q-vector formulation [*Pollard and Regier*, 1992]:

$$f^2\frac{\partial^2\omega}{\partial z^2}+\left(\frac{\partial^2}{\partial x^2}+\frac{\partial^2}{\partial y^2}\right)\left(N^2\omega\right)=\nabla_h Q \tag{1}$$

$$Q=\left[2f\left(\frac{\partial V}{\partial x}\frac{\partial U}{\partial z}+\frac{\partial V}{\partial y}\frac{\partial V}{\partial z}\right),-2f\left(\frac{\partial U}{\partial x}\frac{\partial U}{\partial z}+\frac{\partial U}{\partial y}\frac{\partial V}{\partial z}\right)\right], \tag{2}$$

where f is the Coriolis parameter. The horizontal geostrophic velocity components (U,V) and the Brunt-Väisälä frequency (N) were both estimated from the monthly ARMOR3D (see section 2.1), and ω represents QG-w.

The equation is solved in a three-dimensional domain assuming boundary conditions of QG-w = 0 at the bottom and surface. Neumann conditions are assumed at the lateral boundaries (see details in *Pinot et al*. [1996]). As has been shown in previous studies [e.g., *Rodríguez et al*., 2001; *Pascual et al*., 2004], QG-w was not found to be significantly dependent on the choice of lateral boundary conditions.

2.4. Ekman Vertical Velocities

Ekman upwelling/downwelling associated with average wind stress curl was estimated from the Scatterometer Climatology of Ocean Winds, which is constructed from 122 months (September 1999–October 2009) of QuikSCAT scatterometer data [*Risien and Chelton*, 2008].

2.5. NPP Analytical Model

The analytical model used here to estimate NPP was first proposed by L11. The model considers two layers: a surface (euphotic) layer of depth H (deeper than the upper mixed layer), characterized by phytoplankton concentration P and by nutrients N, and a subsurface nutrient reservoir characterized by phytoplankton and nutrient concentrations P_{sub} and N_{sub}, respectively (the latter being constant over time). These layers interact through two mechanisms: (1) the cumulative impact of (sub) mesoscale vertical exchanges at the base of the euphotic layer, expressed as a vertical flux $-\alpha(C-C_{\mathrm{sub}})$, with C representing either N or P, and α being an estimate of the strength of the vertical turbulence (defined similar to *Lévy et al*. [2010] as the RMS of QG-w), and (2) a background wind-driven upwelling/downwelling at large-scale, represented by a constant, positive/negative w_{Ek}. The biological model includes phytoplankton production (μNP), where μ is the growth rate in units day^{-1}, and loss due to mortality (mP) where m is a constant mortality rate, also in units day^{-1}. A fraction (γ) of mP is remineralized in the euphotic layer, while the remaining part is exported to the subsurface layer.

Finally, the model assumes efficient consumption of the upwelled nutrients in the euphotic layer ($N<<N_{\mathrm{sub}}$) and rapid death of phytoplankton organisms away from the euphotic layer. All these assumptions lead to the following two sets of equations, depending on the sign of the background fluxes. For an upward background vertical flux (i.e., Ekman upwelling as is observed in the Gulf Stream region) [see *Risien and Chelton*, 2008, Figure 7], the analytical model is formulated as follows:

$$\frac{\mathrm{d}N}{\mathrm{d}t}=-\mu NP+\gamma mP+\frac{\alpha+w_{\mathrm{Ek}}}{H}N_{\mathrm{sub}} \tag{3}$$

$$\frac{\mathrm{d}P}{\mathrm{d}t}=\mu NP-mP-\frac{\alpha}{H}P. \tag{4}$$

In the case of downward background vertical fluxes, as is the case for large-scale Ekman downwelling observed in the subtropical oligotrophic gyres [*Risien and Chelton*, 2008], the analytical model becomes

$$\frac{\mathrm{d}N}{\mathrm{d}t}=-\mu NP+\gamma mP+\frac{\alpha}{H}N_{\mathrm{sub}} \tag{5}$$

$$\frac{\mathrm{d}P}{\mathrm{d}t}=\mu NP-mP-\frac{\alpha+w_{\mathrm{Ek}}}{H}P. \tag{6}$$

©2014. American Geophysical Union. All Rights Reserved.

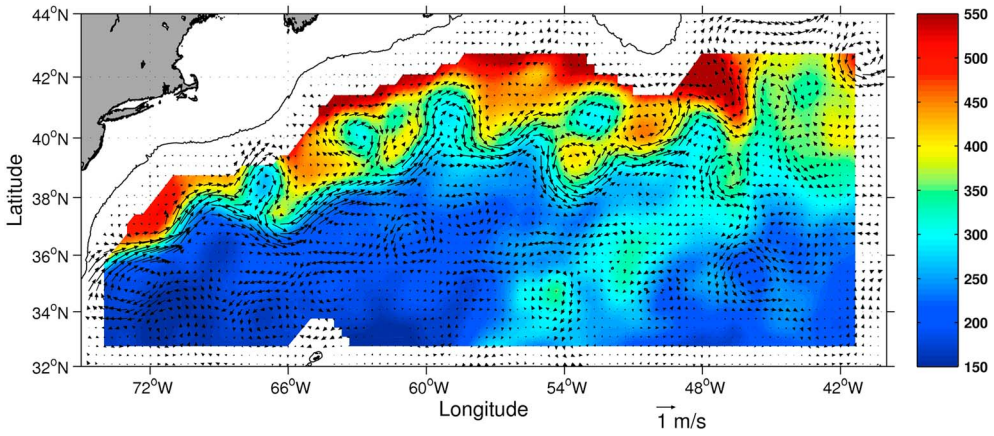

Figure 1. Map of geostrophic surface currents derived from ARMOR3D data for September 2005. The color map corresponds to the monthly mean of net primary production (mg C $m^{-2} d^{-1}$) for the same month. Isolines correspond to 0 and 1000 m isobaths. Areas shallower than 1000 m (bottom boundary in the QG-w computation) have been masked.

Defining NPP as μNP-mP, different expressions relating NPP to the mesoscale vertical flux strength α can thus be obtained. In the case of a positive upward background flux (Ekman upwelling), the relation for NPP is obtained by finding the equilibrium solution of equations (3)–(4):

$$\mathrm{NPP} = \mu NP - mP = \frac{\alpha}{H} P = \frac{N}{H} \frac{\alpha^2 + \alpha w_{\mathrm{Ek}}}{\alpha + w_c}, \tag{7}$$

where w_c is the critical velocity defined as $w_c = (1-\gamma)mH$, which represents export to the deep ocean. Similarly, in the case of large-scale average downward Ekman flux (e.g., in the center of the oligotrophic gyres), the relation for NPP is obtained by finding the equilibrium solution of equations (5) and (6):

$$\mathrm{NPP} = \mu NP - mP = \frac{\alpha + w_{\mathrm{Ek}}}{H} P = \frac{N}{H} \frac{\alpha^2 + \alpha w_{\mathrm{Ek}}}{\alpha + w_c - w_{\mathrm{Ek}}}. \tag{8}$$

One of the limitations of the L11 model is that it is only valid when the mixed layer is shallower than the euphotic layer. As such, this study is limited to the summer, when such conditions are observed in the North Atlantic.

3. Results

The geostrophic fields derived from ARMOR3D at 100 m, which is considered the limit for the average euphotic layer in the area [*Oschlies and Garçon*, 1998], reveal the presence of the most distinctive structures of this area, that is, the Gulf Stream jet and numerous mesoscale eddies of diameter around 200 km (see snapshot in Figure 1). Maximum velocities are found in the jet with values of around 1 m s^{-1}. Using the scale values $U = 1$ m s^{-1}, $f = 10^{-4}$ s^{-1}, and L (half diameter) = 100 km, we obtain a value of about 0.1 for the Rossby number, which justifies the QG analysis presented below.

A general northward gradient in NPP is well depicted by the snapshot shown in Figure 1. This latitudinal gradient is likely a result of numerous factors, including the nutricline depth (stratification), changes in phytoplankton community composition, and changes in the ambient light field in combination with a response to mesoscale dynamics [*Siegel et al.*, 1999]. The background, large-scale gradient in NPP is augmented by mesoscale eddies and meanders, as revealed in detail in Figure 1. Cyclonic eddies, presumably formed from the pinching off of Gulf Stream meanders, can be observed south of the Gulf Stream appearing to trap and maintain high NPP relative to their surroundings.

While eddies can be easily shown to be effective mechanism for tracer (and phytoplankton) redistribution through horizontal advection [e.g., *Lehahn et al.*, 2011; *D'Ovidio et al.*, 2013; *Gaube et al.*, 2014], additional mechanisms are required to sustain the nutrient fluxes inside the eddies, namely vertical exchanges across the

©2014. American Geophysical Union. All Rights Reserved.

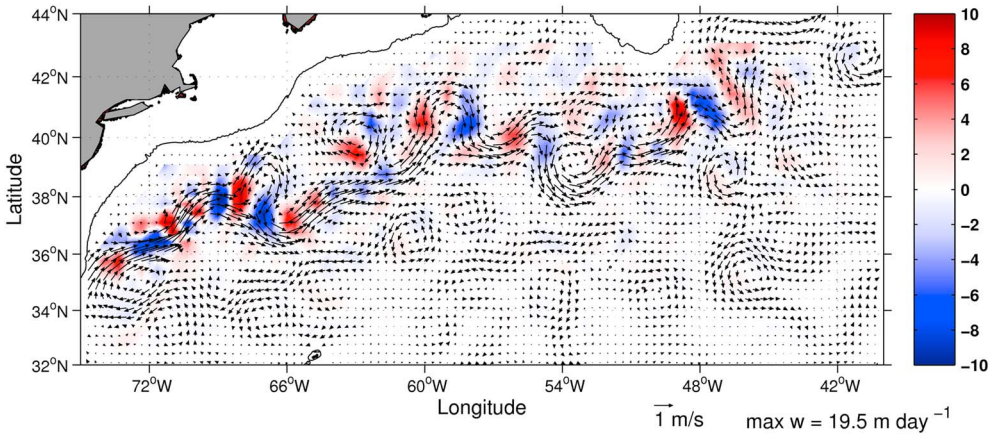

Figure 2. Map of vertical velocity (m d^{-1}) at 100 m, obtained by integrating the QG omega equation from the 3-D field of ARMOR3D data corresponding to September 2005. Horizontal geostrophic currents are superimposed. Areas shallower than 1000 m (bottom boundary in the QG-w computation) are masked.

base of the euphotic layer. Indeed, intense vertical motion takes place along the jet, upstream/downstream of meander troughs, and within the mesoscale eddies, where multipolar vertical velocity patterns are generally observed (Figure 2). Maximum upwelling/downwelling reaches up to 20 m d^{-1} (0.23 mm s^{-1}) in the Gulf Stream associated instabilities. In the subtropical gyre, QG-w decreases significantly down to 1–2 m d^{-1}.

To first approximation, the dipoles of positive and negative vertical velocities around meanders are explained by conservation of potential vorticity [*Pollard and Regier*, 1992]. For the case of an anticyclonic meander, water upstream of the meander crest experiences a decrease in relative vorticity and a commiserate decrease in the thickness between isopycnal layers, resulting in upwelling. Downstream of the crest, relative vorticity increases generating downwelling as a result of increased thickness of the isopycnal surfaces. The opposite occurs in cyclonic meanders, with downwelling and upwelling located upstream and downstream of the cyclonic meander, respectively.

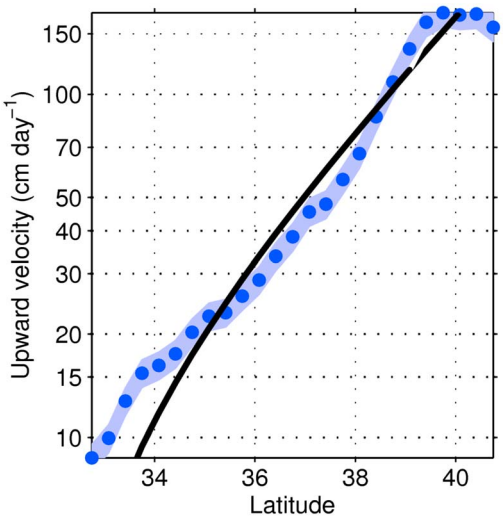

Figure 3. Meridional section of upward QG-w (cm d^{-1}), averaged from 65°W to 40°W and over the 1998–2009 period (logarithmic scale). The 95% confidence interval is shaded in light blue (error estimated using a chi-square test), and the black line corresponds to the fitted trend.

These structures agree with the patterns obtained by *Gomis et al.* [2005] using the simplified QG model of baroclinic instability proposed by *Tang* [1975]. Similar dipoles of QG-w have also been retrieved from in situ observations around a meander in the Northwestern Mediterranean [*Pascual et al.*, 2004].

Similarly, the multipolar vertical velocity patterns observed in the mesoscale eddies [e.g., *Martin and Richards*, 2001; *Pidcock et al.*, 2013] can be explained as the azimuthal propagation of potential vorticity (PV) disturbances along the radial gradient of PV associated with the basic state eddy, known in the literature as vortex Rossby waves [*Buongiorno Nardelli*, 2013].

The averaged upward QG-w increases exponentially with latitude (Figure 3). This pattern can be explained by a simple model, assuming that upward (note that equivalent results are obtained for the

©2014. American Geophysical Union. All Rights Reserved.

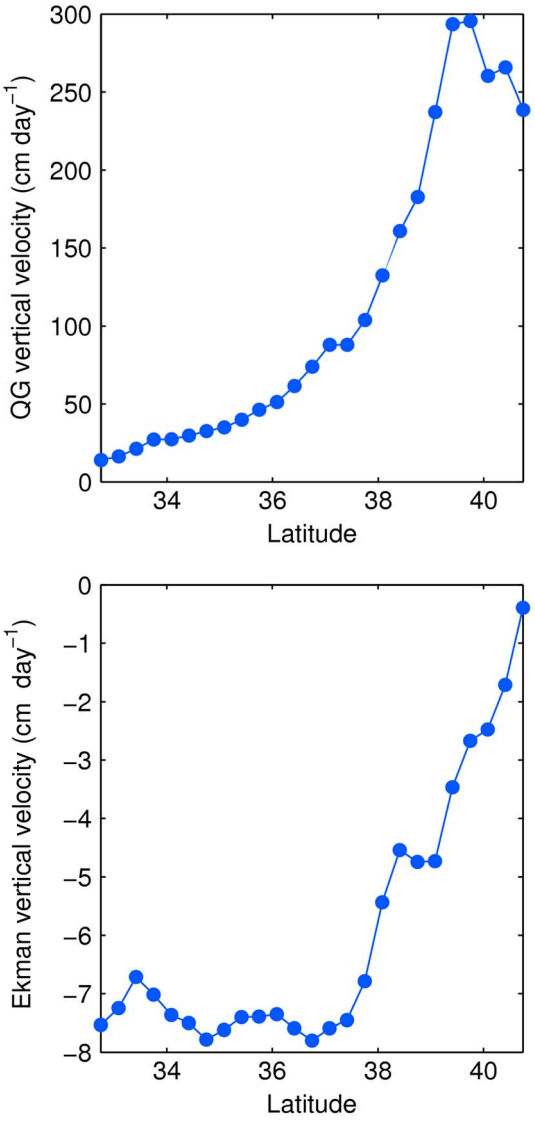

Figure 4. Vertical velocity inputs for the application of the L11 model, as a function of latitude, over the same zone and period as in Figure 3 but only for summer season: (top) RMS of QG-w at 100 m (cm d^{-1}); (bottom) climatological Ekman vertical velocity (cm d^{-1}).

downward component as well) QG-w is locally proportional to the intensity of the mesoscale structures, which are created at the core of the Gulf Stream (by baroclinic and other instabilities) and then diffused away by stochastic processes (e.g., eddy-eddy interactions, etc.) while damped by friction with deeper layers and by atmospheric forcing on a specific time scale. Thus, the distribution of QG-w can be described using a 2-D advection-diffusion equation, adding a simple relaxation term (see supporting information for details). Fitting $<$QG-w$>$ with an exponential function gives an *e*-folding scale of 300 km which, in turn gives 100–200 days as a relaxation time scale for the mesoscale structures, assuming a $K = 5000–10000\ m^2/s$ [*Abernathey and Marshall*, 2013]. This is a very qualitative, yet interesting, result, since it provides a tight observational constraint on quantities that are generally elusive. It also suggests that, basically, the whole area is driven by the same physical process, which is not obvious, considering distance from the source region (the Gulf Stream) and the possibility that other mechanisms can act as sources for the mesoscale variability (e.g., wind forcing or westward Rossby waves).

In order to investigate the net effects of mesoscale turbulence and basin-scale Ekman vertical fluxes on NPP, we apply the L11 model described in section 2.5 by using average *N*, $<$RMS(QG-w)$>$ (Figure 4, top), and w_{Ek} (Figure 4, bottom) to estimate NPP from equations (3)–(6). We then vary the only free parameter of the L11 model, the critical upwelling velocity (w_c), between 1 and 3 m/d^{-1} to obtain a best fit approximation of observed NPP.

Figure 5 shows that observed NPP values in the vicinity of the Gulf Stream (high-latitude band in the figure) are within the range of values predicted by the conceptual model. These results are robust and consistent, independent of the NPP product used. Conversely, the analytical model indicates that vertical motions driven by mesoscale turbulence are not able to support the level of NPP observed along the northern flank of the North Atlantic subtropical gyre, regardless of choice of w_c (Figure 5). This is due mostly to the low-nutrient concentration at the base of the euphotic layer (the nutricline deepens significantly south of 38°N) and also to the weaker mesoscale vertical exchanges (Figure 4, top). The basin-scale Ekman downwelling (w_{Ek}) has a negligible role with respect to QG-w in setting NPP values. Sensitivity tests revealed that even after artificially increasing the climatological w_{Ek} downwelling velocity by a factor of 4, observed NPP was not reproduced by the L11 model south of 38°N in the study region. This points to the inadequacy of models based only on mesoscale vertical nutrient fluxes across the base of the euphotic zone (and mean nutrient distribution) to describe North Atlantic dynamics.

©2014. American Geophysical Union. All Rights Reserved.

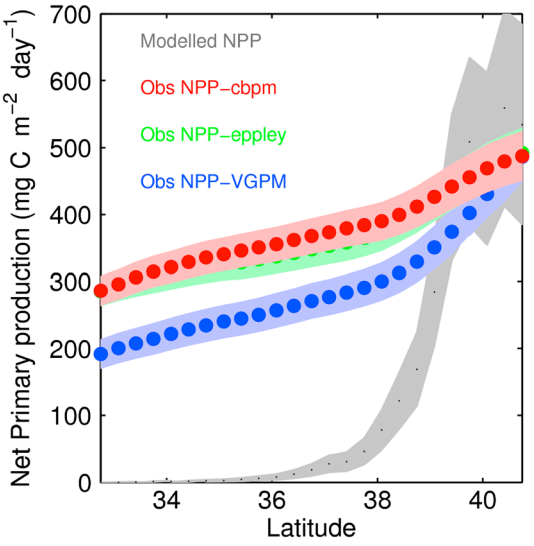

Figure 5. Observed mean NPP (from NPP-VGPM, Eppley, and cbpm) versus modeled mean NPP as a function of latitude. The average has been estimated in the range of longitudes from 65°W to 40°W and over 1998–2009 period (only for the summer season: July, August, and September). The 95% confidence interval is shaded for the observed products (error estimated using a chi-square test). The modeled grey band represents the dispersion of mean NPP by using values of w_c between 1 and 3 m d^{-1}.

4. Discussion and Conclusions

Our results suggest that mesoscale regions of upwelling and downwelling impact primary production in the Gulf Stream region, where the local supply of nutrients and their remote advection are believed to play a critical role in sustaining the biological pump. Mesoscale upwelling and downwelling is largest in magnitude in the vicinity of Gulf Stream meanders and eddies. These mesoscale vertical velocities can be diffused away from the Gulf Stream region following stochastic processes, as shown by the analysis of a simple damped diffusion/advection equation. The patterns of QG-w are not only consistent with those retrieved in other studies applying the QG framework in other areas of the Global Ocean [e.g., *Pollard and Regier*, 1992; *Pascual et al*., 2004; *Buongiorno Nardelli*, 2013] but also comparable with model results and indirect estimates in the Gulf Stream [*Osgood et al*., 1987; *Anderson and Robinson*, 2001].

We have investigated the latitudinal gradient of mesoscale vertical velocity variability and its relation with NPP. In fact, though one might expect QG-w to be important in advecting nutrients from the deeper layers all along the latitudinal range considered, its efficiency is highly dependent on the quantity of nutrients that can effectively enter the euphotic layer, so that other mechanisms are needed to explain observed levels of NPP along the northern flank of the North Atlantic subtropical gyre.

Submesoscale dynamics may play a role, as recently suggested by *Lévy et al*. [2014] using a high-resolution model tuned for the North Atlantic. Figure 2b of this study reveals a vertical velocity field extremely similar to our patterns in the area of the Gulf Stream both in intensity and shape. This further confirms that our results are consistent with model data and that mesoscale dynamics is dominant. On the contrary, more to the south, where our QG estimates lead to very weak vertical motion (1–2 m d^{-1}), the w patterns in *Lévy et al*. [2014] are related to submesoscale filament features with considerably larger maximum values (10 m d^{-1}). However, even increasing by a factor 5 the QG-w used in L11, though improving the modeled NPP, we could not reproduce satellite NPP levels in the center of the subtropical gyre, most probably due to the very deep nutricline in that area.

As a consequence, horizontal advection might be critical in the intergyre regions of the open ocean where a significant nutrient flux from the polar gyre fertilizes the boundary of the subtropical gyre [*Oschlies*, 2002; *Palter et al*., 2005]. Furthermore, the mesoscale eddies that originate in the Gulf Stream may effectively redistribute phytoplankton horizontally, as they can transport properties in their cores for long periods of time [*Lehahn et al*., 2011; *D'Ovidio et al*., 2013].

The availability of the global ARMOR3D product enables the application of the methods presented in this study to other parts of the World Oceans. Furthermore, it is expected that in the future, with the advent of swath altimetry [*Fu and Ubelmann*, 2013] together with sustained Argo and the global in situ ocean observing system [*Le Traon*, 2013], similar analyses will be routinely possible at higher temporal and spatial resolutions.

4.1. Availability of the Data

The fields of QG-vertical velocities described in this paper are saved in Matlab format and are available from the first author upon request.

©2014. American Geophysical Union. All Rights Reserved.

Acknowledgments

This work has been carried out as part of MESCLA (PB-LC 10–013) and E-MOTION (CTM2012-31014) projects, funded within the Open Call for R&D activities in the framework the MyOcean project (EU FP7-SPACE-2007-1-grant agreement 218812) and the Spanish National Research Program, respectively. A.P. gratefully acknowledges Peter Gaube and Dennis J. McGillicuddy Jr. for stimulating discussions and meaningful suggestions during her visit to Woods Hole Oceanographic Institution. The manuscript was improved by the comments of two anonymous reviewers and by editorial revisions of P. Gaube and E. Mason. The ARMOR-3D data set was produced by CLS with support from MyOcean project. Net primary production data were obtained from Oregon State University (Ocean Productivity). Nitrate data were extracted from World Ocean Atlas (WOA) climatology.

The Editor thanks two anonymous reviewers for their assistance in evaluating this paper.

References

Abernathey, R. P., and J. Marshall (2013), Global surface eddy diffusivities derived from satellite altimetry, *J. Geophys. Res. Oceans*, *118*, 901–916, doi:10.1002/jgrc.20066.

Allen, J. T., D. A. Smeed, J. Tintoré, and S. Ruiz (2001), Mesoscale subduction at the Almeria-Oran front. Part 1: Ageostrophic flow, *J. Mar. Syst.*, *30*, 263–285, doi:10.1016/S0924-7963(01)00062-8.

Anderson, L. A., and A. R. Robinson (2001), Physical and biological modeling in the Gulf Stream region Part II. Physical and biological processes, *Deep Sea Res., Part I*, *48*(2001), 1139–1168.

Behrenfeld, M. J., and P. G. Falkowski (1997), Photosynthetic rates derived from satellite-based chlorophyll concentration, *Limnol. Oceanogr.*, *42*, 1–20.

Benítez-Barrios, V. M., et al. (2011), Three-dimensional circulation in the NW Africa coastal transition zone, *Prog. Oceanogr.*, *91*(4), 516–533.

Boyer, T. P., et al. (2009), *World Ocean Database 2009*, *NOAA Atlas NESDIS*, vol. 66, edited by S. Levitus, pp. 216, U.S. Gov. Printing Office, Washington, D. C., DVDs.

Buongiorno Nardelli, B. (2013), Vortex waves and vertical motion in a mesoscale cyclonic eddy, *J. Geophys. Res. Oceans*, *118*, 5609–5624, doi:10.1002/jgrc.20345.1.

Buongiorno Nardelli, B., S. Sparnocchia, and R. Santoleri (2001), Small mesoscale features at a meandering upper ocean front in the western Ionian Sea (Mediterranean Sea): Vertical motion and potential vorticity analysis, *J. Phys. Oceanogr.*, *31*(8), 2227–2250.

Buongiorno Nardelli, B., S. Guinehut, A. Pascual, Y. Drillet, S. Ruiz, and S. Mulet (2012), Towards high resolution mapping of 3-D mesoscale dynamics from observations, *Ocean Sci.*, *8*, 885–901.

Calil, P. H. R., and K. J. Richards (2010), Transient upwelling hot spots in the oligotrophic North Pacific, *J. Geophys. Res.*, *115*, C02003, doi:10.1029/2009JC005360.

Chelton, D. B., P. Gaube, M. G. Schlax, J. J. Early, and R. M. Samelson (2011), The influence of nonlinear mesoscale eddies on near-surface oceanic chlorophyll, *Science*, *334*, 328–332.

Cunningham, S. A., et al. (2007), Temporal variability of the Atlantic meridional overturning circulation at 26.51N, *Science*, *317*(5840), 935–938, doi:10.1126/science.1141304.

D'Ovidio, F., S. De Monte, A. D. Penna, C. Cotté, and C. Guinet (2013), Ecological implications of eddy retention in the open ocean: A Lagrangian approach, *J. Phys. A: Math. Theor.*, *46*(25), 254023.

Ferry, N., L. Parent, G. Garric, B. Barnier, N. C. Jourdain, and the Mercator Ocean team (2010), Mercator global eddy permitting ocean reanalysis GLORYS1V1: Description and results, *Mercator Ocean Q. Newsl.*, *36*, 15–27.

Franks, P. J. S., J. Wroblewski, and G. R. Flierl (1986), Prediction of phytoplankton growth in response to the frictional decay of a warm-core ring, *J. Geophys. Res.*, *91*(C6), 7603–7610, doi:10.1029/JC091iC06p07603.

Fu, L.-L., and C. Ubelmann (2013), On the transition from profile altimeter to swath altimeter for observing global ocean surface topography, *J. Atmos. Oceanic Technol.*, doi:10.1175/JTECH-D-13-00109.1.

Gaube, P., D. B. Chelton, P. G. Strutton, and M. J. Behrenfeld (2013), Satellite observations of chlorophyll, phytoplankton biomass, and Ekman pumping in nonlinear mesoscale eddies, *J. Geophys. Res. Oceans*, *118*, 6349–6370, doi:10.1002/2013JC009027.

Gaube, P., D. J. McGillicuddy, D. B. Chelton, M. J. Behrenfeld, and P. G. Strutton (2014), Regional variations in the influence of mesoscale eddies on near-surface chlorophyll, *J. Geophys. Res. Oceans*, *119*, doi:10.1002/2014JC010111.

Gomis, D., S. Ruiz, and M. A. Pedder (2001), Diagnostic analysis of the 3D ageostrophic circulation from a multivariate spatial interpolation of CTD and ADCP data, *Deep Sea Res., Part I*, *48*, 269–295.

Gomis, D., A. Pascual, and M. A. Pedder (2005), Errors in dynamical fields inferred from oceanographic cruise data: Part II. The impact of the lack of synopticity, *J. Mar. Syst.*, *56*, 334–351.

Gonzalez-Quiros, R., A. Pascual, D. Gomis, and R. Anadon (2004), Influence of mesoscale physical forcing on trophic pathways and fish larvae retention in the central Cantabrian Sea, *Fish. Oceanogr.*, *13*(6), 351–364.

Guinehut, S., P.-Y. Le Traon, G. Larnicol, and S. Philipps (2004), Combining Argo and remote-sensing data to estimate the ocean three-dimensional temperature fields—A first approach based on simulated observations, *J. Mar. Syst.*, *46*(1–4), 85–98.

Guinehut, S., A. L. Dhomps, G. Larnicol, and P. Y. Le Traon (2012), High resolution 3-D temperature and salinity fields derived from in situ and satellite observations, *Ocean Sci.*, *8*, 845–857.

Gruber, N., Z. Lachkar, H. Frenzel, P. Marchesiello, M. Münnich, J. C. McWilliams, T. Nagai, and G. K. Plattner (2011), Eddy-induced reduction of biological production in eastern boundary upwelling systems, *Nat. Geosci.*, *4*, 787–792.

Klein, P., and G. Lapeyre (2009), The oceanic vertical pump induced by mesoscale eddies, *Annu. Rev. Mar. Sci.*, *1*, 351–375.

Lathuiliere, C., M. Levy, and V. Echevin (2011), Impact of eddy-driven vertical fluxes on phytoplankton abundance in the euphotic layer, *J. Plankton Res.*, *33*, 827–831, doi:10.1093/plankt/fbq131.

Le Traon, P. Y. (2013), From satellite altimetry to Argo and operational oceanography: Three revolutions in oceanography, *Ocean Sci.*, *9*, 901–915.

Lehahn, Y., F. D'Ovidio, M. Lévy, Y. Amitai, and E. Heifetz (2011), Long range transport of a quasi isolated chlorophyll patch by an Agulhas ring, *Geophys. Res. Lett.*, *38*, L16610, doi:10.1029/2011GL048588.

Lévy, M., P. Klein, and A.-M. Treguier (2001), Impact of sub-mesoscale physics on production and subduction of phytoplankton in an oligotrophic regime, *J. Mar. Res.*, *59*, 535–565, doi:10.1357/002224001762842181.

Lévy, M., P. Klein, A. M. Tréguier, D. Iovino, G. Madec, S. Masson, and K. Takahashi (2010), Modifications of gyre circulation by sub-mesoscale physics, *Ocean Modell.*, *34*, 1–15.

Lévy, M., O. Jahn, S. Dutkiewicz, and M. J. Follows (2014), Phytoplankton diversity and community structure affected by oceanic dispersal and mesoscale turbulence, *Limnol. Oceanogr.: Fluids Environ.*, *4*, 67–84, doi:10.1215/21573689-2768549.

Lique, C., G. Garric, A. Treguier, B. Barnier, N. Ferry, C. Testut, and F. Girard-Ardhuin (2011), Evolution of the Arctic Ocean salinity, 2007–08: Contrast between the Canadian and the Eurasian Basins, *J. Clim.*, *24*(6), 1705–1717, doi:10.1175/2010JCLI3762.1.

Mahadevan, A. (2014), Ocean science: Eddy effects on biogeochemistry, *Nature*, *506*, 168–169, doi:10.1038/nature13048.

Mahadevan, A., and A. Tandon (2006), An analysis of mechanisms for submesoscale vertical motion at ocean fronts, *Ocean Modell.*, *14*, 241–256.

Mahadevan, A., E. D'Asaro, C. Lee, and M. J. Perry (2012), Eddy-driven stratification initiates North Atlantic spring phytoplankton blooms, *Science*, *336*, 54–58.

Martin, A. P., and K. J. Richards (2001), Mechanisms for vertical nutrient transport within a North Atlantic mesoscale eddy, *Deep Sea Res., Part II*, *48*, 757–773, doi:10.1016/S0967-0645(00)00096-5.

McGillicuddy, D. J., Jr., A. R. Robinson, D. A. Siegel, H. W. Jannasch, R. Johnson, T. D. Dickey, J. McNeil, A. F. Michaels, and A. H. Knap (1998), Influence of mesoscale eddies on new production in the Sargasso Sea, *Nature*, *394*, 263–266, doi:10.1038/28367.

©2014. American Geophysical Union. All Rights Reserved.

McGillicuddy, D. J., et al. (2007), Eddy/wind interactions stimulate extraordinary mid-ocean plankton blooms, *Science*, *316*(5827), 1021–1026.
Mulet, S., M. H. Rio, A. Mignot, S. Guinehut, and R. Morrow (2012), A new estimate of the global 3D geostrophic ocean circulation based on satellite data and in-situ measurements, *Deep Sea Res., Part II*, *77–80*, 70–81.
Naveira Garabato, A. C., J. T. Allen, H. Leach, V. H. Strass, and R. T. Pollard (2001), Mesoscale subduction at the Antarctic Polar Front driven by baroclinic instability, *J. Phys. Ocean.*, *31*, 2087–2107.
Oschlies, A. (2002), Nutrient supply to the surface waters of the North Atlantic: A model study, *J. Geophys. Res.*, *107*(C5), 3046, doi:10.1029/2000JC000275.
Oschlies, A., and V. Garçon (1998), Eddy-induced enhancement of primary production in a model of the North Atlantic Ocean, *Nature*, *394*, 266–269.
Osgood, K. E., J. M. Bane Jr., and W. K. Dewar (1987), Vertical velocities and dynamical balances in Gulf Stream meanders, *J. Geophys. Res.*, *92*(C12), 13,029–13,040, doi:10.1029/JC092iC12p13029.
Palter, J. B. M., S. Lozier, and R. T. Barber (2005), The effect of advection on the nutrient reservoir in the North Atlantic subtropical gyre, *Nature*, *437*, doi:10.1038/nature03969.
Pascual, A., D. Gomis, R. L. Haney, and S. Ruiz (2004), A quasigeostrophic analysis of a meander in the Palamos Canyon: Vertical velocity, geopotential tendency, and a relocation technique, *J. Phys. Oceanogr.*, *34*(10), 2274–2287.
Pidcock, R., A. Martin, J. T. Allen, S. C. Painter, and D. Smeed (2013), The spatial variability of vertical velocity in an Iceland basin eddy dipole, *Deep Sea Res., Part I*, *72*, 121–140, doi:10.1016/j.dsr.2012.10.008.
Pinot, J. M., J. Tintoré, and D. P. Wang (1996), A study of the omega equation for diagnosing vertical motions at ocean fronts, *J. Mar. Res.*, *54*(2), 239–259.
Pollard, R. T., and L. A. Regier (1992), Vorticity and vertical circulation at an ocean front, *J. Phys. Oceanogr.*, *22*, 609–625.
Risien, C. M., and D. B. Chelton (2008), A global climatology of surface wind and wind stress fields from eight years of QuikSCAT scatterometer data, *J. Phys. Oceanogr.*, *38*, 2379–2413.
Rodríguez, J., J. Tintoré, J. T. Allen, J. Blanco, D. Gomis, A. Reul, J. Ruiz, V. Rodríguez, F. Echevarría, and F. Jiménez-Gómez (2001), The role of mesoscale vertical motion in controlling the size structure of phytoplankton in the ocean, *Nature*, *410*, 360–363.
Ruiz, S., A. Pascual, B. Garau, I. Pujol, and J. Tintoré (2009), Vertical motion in the upper ocean from glider and altimetry data, *Geophys. Res. Lett.*, *36*, L14607, doi:10.1029/2009GL038569.
Siegel, D. A., E. Fields, and D. J. McGillicuddy Jr. (1999), Mesoscale motions, satellite altimetry and new production in the Sargasso Sea, *J. Geophys. Res.*, *104*, 13,359–13,379, doi:10.1029/1999JC900051.
Siegel, D. A., D. B. Court, D. W. Menzies, P. Peterson, S. Maritorena, and N. B. Nelson (2008), Satellite and in situ observations of the bio-optical signatures of two mesoscale eddies in the Sargasso Sea, *Deep Sea Res., Part II*, *55*, 1218–1230, doi:10.1016/j.dsr2.2008.01.012.
Tang, C. (1975), Baroclinic instability of stratified shear flow in the ocean and atmosphere, *J. Geophys. Res.*, *80*, 1168–1175, doi:10.1029/JC080i009p01168.
Tintoré, J., D. Gomis, S. Alonso, and G. Parrilla (1991), Mesoscale dynamics and vertical motion in the Alboran Sea, *J. Phys. Oceanogr.*, *21*, 811–823.
Viúdez, A., and M. Claret (2009), Numerical simulations of submesoscale balanced vertical velocity forcing unsteady nutrient-phytoplankton-zooplankton distributions, *J. Geophys. Res.*, *114*, C04023, doi:10.1029/2008JC005172.
Westberry, T., M. J. Behrenfeld, D. A. Siegel, and E. Boss (2008), Carbon-based primary productivity modeling with vertically resolved photoacclimation, *Global Biogeochem. Cycles*, *22*, GB2024, doi:10.1029/2007GB003078.

©2014. American Geophysical Union. All Rights Reserved.